



Contents lists available at ScienceDirect

Journal of Power Sources

journal homepage: www.elsevier.com/locate/jpowsour

Exploration of unalloyed bimetallic Au–Pt/C nanoparticles for oxygen reduction reaction

S. Senthil Kumar*, K.L.N. Phani

Electrodics and Electrocatalysis Division, Central Electrochemical Research Institute, Karaikudi 630 006, India

ARTICLE INFO

Article history:

Received 13 August 2008

Received in revised form 28 August 2008

Accepted 15 October 2008

Available online 8 November 2008

Keywords:

Unalloyed Au–Pt/C bimetallic nanoparticle

Oxygen reduction

Methanol oxidation

Rotating disc electrode

ABSTRACT

The synthesis of carbon-supported unalloyed Au–Pt bimetallic nanoparticles using polyol method at a temperature as low as 85 °C is reported. Various compositions of Au–Pt/C bimetallic nanoparticles are characterized using transmission electron microscopy (TEM), X-ray fluorescence (XRF), X-ray diffraction and cyclic voltammetry. Electron microscopy shows that the particles have a near-narrow size distribution that peaks at an average size of ~5 to 6 nm. The electrocatalytic activity of Au–Pt/C nanoparticles towards the oxygen reduction reaction (ORR) is studied by linear sweep polarization measurements obtained using a rotating disc electrode (RDE). The results reveal that a four-electron transfer pathway is mainly operative for ORR and the half-wave potential for ORR on bimetallic Au–Pt/C (20%:20%) is ~100 mV less negative when compared with that of Pt/C (home-made and E-Tek). Studies of the methanol oxidation reaction (MOR) on these catalysts show that the MOR activity is significantly lowered with increasing content of Au in Au–Pt/C.

© 2008 Elsevier B.V. All rights reserved.

1. Introduction

Bimetallic nanoparticles are particularly attractive due to an improvement in the catalytic properties relative to the separate metals [1,2]. As a continuing effort to screen electrocatalysts for fuel cell reactions, the results obtained from studies of the combination of gold with platinum in the form of nanoparticles supported on porous carbon are discussed in this work. An important step in understanding how this combination works is the realization that the Pt–Au pair is able to form homogeneous alloy particles, provided their size is not greater than about 3 nm, in spite of the fact that in the bulk state there is a wide miscibility gap. The Pt–Au combination has also proved to be beneficial; it performs better than platinum alone in: (i) oxygen reduction at a fuel cell cathode [3]; (ii) selective oxidation of reducing sugars and other polyols [4]; (iii) alkane isomerisation, when contained in the cages of the HY zeolite structure [5]; (iv) reactions of environmental importance such as nitric oxide reduction by propene [4].

The choice of Pt–Au system is based on: (i) the wealth of information available in literature; (ii) the question of how synthetic procedures affect the structural characteristics that contribute to catalytic activity; (iii) the possibility that Au and Pt can play a synergistic role in fuel cell reactions, for example, the methanol oxidation

reaction (MOR) and the oxygen reduction reaction (ORR) in acid solutions. Based on simple thermodynamic principles, Fernandez et al. [6] provided guidelines for the design of binary and multi-component electrocatalytic materials for the reduction of oxygen, which combine one metal that easily breaks the O–O bond of O₂ (forming adsorbed atomic oxygen) with another metal that will easily reduce adsorbed atomic oxygen. Some of the most efficient catalyst systems these authors have proposed are gold-based and these were subsequently pursued by Manthiram et al. [7].

The driving force for selecting Au–Pt is provided by the following observations made in the published literature, namely: (i) the presence of Au in Pt increases the lattice distance of Pt; (ii) the higher electronegativity of Au than Pt can cause an increase of the amount of charge transferred from Pt to Au, which in fact derives support from high resolution XPS data that shows a Au 4f_{7/2} binding energy of 83.32 eV for Au–Pt and 83.87 eV for bulk Au atoms [8] and, consequently, an increase in the d-orbital vacancy in Au–Pt. It is believed that there exists a balance of Pt-site activation of O₂ via dissociation and Au-site promotion by –OH adsorption [9]. These aspects imply a bifunctional activity of Au–Pt towards, for example, the ORR. The formation of Au–OH is operative for an alloy catalyst with 60–80% Au atoms surrounding Pt in chemisorption of the reaction intermediate from O₂ dissociation at Pt via formation of HO₂[–]_{ad}, and such species should have sufficient binding strength with Au in a further 2e[–] reduction to H₂O. In addition, gold nanoparticles have been found to be good catalysts for CO oxidation and methanol oxidation reaction in alkaline media, especially when Pt is part of

* Corresponding author. Tel.: +91 4565 227550; fax: +91 4565 227779.
E-mail address: ssenthilmugam@gmail.com (S. Senthil Kumar).

the catalyst. However, the reaction pathways, and hence the rates, depend significantly on the composition and the type of bimetallic system, i.e., alloyed or unalloyed. In this, choice of the preparative method has played an important role in controlling the composition and the phase of the catalyst.

In a different vein, Adzic et al. [10] reported enhancement of ORR activity by placing Au clusters on the platinum surface. Via an electronic effect, this appears to minimize the dissolution of Pt in the electrolyte. In explaining the enhanced activity for ORR, the authors considered an efficient spill-over of H_2O_2 from the Au clusters to the surrounding Pt atoms, where further reduction to H_2O can take place.

The polyol method and its modified versions have been employed for the synthesis of nanoparticles of Pt–Ru, Pt–M (M = V, Ni, Cr, Co, and Fe) and palladium-based bimetallics. This method involves co-reduction of the metal salts using the acetaldehyde intermediate formed during refluxing of the metal salts in ethylene glycol or its variants, e.g., di- or tetra-ethylene glycols [11–13].

In this work, carbon-supported Au–Pt nanoparticles have been prepared via the polyol method at a temperature as low as 85 °C. The liquid polyol serves as both a solvent and a reducing agent, and it often acts as a protecting agent, preventing particle sintering. Considering the significance of the issue of methanol-tolerance of cathode (oxygen reduction) electrocatalysts in direct methanol fuel cells [14], the premise in this study is that by changing the composition of Au–Pt nanoparticles, it will be possible to understand the extent to which the catalytic activity for both methanol oxidation and oxygen reduction reactions can be controlled. The results obtained for Au–Pt of various compositions with respect to their behaviour towards these two reactions are reported.

2. Experimental procedure

2.1. Chemicals

Hydrogen hexachloroplatinate(IV) ($H_2PtCl_6 \cdot xH_2O$, 99.995%), hydrogen tetrachloroaurate, ($HAuCl_4$, 99%), ethylene glycol (EG), and Nafion®-117 solution (5%) were purchased from Aldrich and used as-received. Vulcan XC 72R was obtained from Cabot Corp. Inc., and sulfuric acid and methanol from E-Merck. All the chemicals are used as-received. All aqueous solutions were prepared in Milli-Q water (18 M Ω , Millipore).

2.2. Synthesis of Au–Pt/C bimetallic nanoparticles

The polyol method was followed to prepare carbon-supported mono- and bi-metallic nanoparticles. Appropriate volumes of $HAuCl_4$ and H_2PtCl_6 solutions were taken in the reaction mixture along with a constant weight of 0.06 g (60%) of Vulcan carbon dissolved in 40 ml ethylene glycol (EG) solution. The resulting solution mixture was allowed to reflux for 4 h at 85 °C. Solid samples of mono- and bi-metallic nanoparticles supported on carbon were separated from the supernatant by centrifugation and subsequently washed three times with both distilled water and acetone in order to remove any organic species produced during the polyol process. Finally, the powders were dried under vacuum at room temperature. Various compositions of Au–Pt/C bimetallic nanoparticles were prepared by varying the atomic ratio of Au and Pt metals salts, while keeping the carbon loading constant at 60 wt.% with total metal loading at 40 wt.%.

2.3. Catalyst coatings on glassy carbon electrode (GCE)

Glassy carbon electrode (geometric area, 0.07 cm²) surfaces were polished using 4/0 grade, alumina-coated, emery paper. A

typical suspension of the catalyst ink was prepared by suspending 2.5 mg of catalyst (Pt/C or Au–Pt/C), 0.125 ml of Nafion solution (5 wt.%) in 0.625 ml of water and then sonicating for 15 min. An aliquot of 3 μ l catalyst ink was then placed on the surface of the polished GCE and dried in air at room temperature.

2.4. Instruments and measurements

2.4.1. Transmission electron microscopy (TEM)

Transmission electron microscopic examination of the samples was carried out with a Philips CM200 microscope operating at 200 kV. The Pt/C or Au–Pt/C samples were dispersed in acetone and then drop-cast on carbon-coated copper grids, followed by solvent evaporation in air at room temperature.

2.4.2. X-ray powder diffraction (XRD)

X-ray diffraction measurements of Pt/C- or Au–Pt/C-supported catalysts were carried out on a Philips PANalytical X-ray diffractometer using Cu K α radiation ($\lambda = 0.15406$ nm). The diffraction angle 2θ was scanned at 0.0170° per step. Each data point was measured for 15 s per 0.1°. Scans were recorded over a 2θ range of 15–90°. Identification of the phases was made by referring to the database of the Joint Committee on Powder Diffraction Standards, International Center for Diffraction Data (JCPDS-ICDD).

2.4.3. Cyclic voltammetry and hydrodynamic voltammetry

Voltammetric and rotating disc electrode experiments were undertaken with a Potentiostat/Galvanostat BAS 100 B (Bioanalytical Systems Inc.) at room temperature. The experiments were performed in a three-electrode electrochemical cell at a room temperature (25 ± 1 °C). For voltammetric studies, a glassy carbon working electrode (BAS) of area: 0.07 cm², a platinum foil counter electrode and a mercury|mercurous sulfate (MSE 0.5 M H_2SO_4) reference electrode were used. All potential values are reported with respect to the MSE (0.5 M H_2SO_4).

3. Results and discussion

The composition of the Au–Pt/C bimetallic nanoparticles was determined by means of X-ray fluorescence (XRF) analysis. It was found that the composition in various parts of the surface is an average of the individual nanoparticles of same category and is close to the nominal value.

The effective atomic weight percentages of the Au and Pt metal, from which the compositions of Au–Pt/C nanoparticles are obtained, are listed in Table 1. The atomic compositions are close to those expected from the content of the two elements employed for the preparation of the bimetallic nanoparticles.

The X-ray powder diffraction patterns of various compositions of Au–Pt/C nanoparticles are presented in Fig. 1. For the sake of comparison, the XRD patterns of individual Au/C (40%) and Pt/C (40%) are also included. Characteristic reflections for Au and Pt, as marked

Table 1
Relative composition of Au–Pt/C obtained from XRF and corresponding electrochemically active surface area of platinum.

Composition (atomic wt.%)	Ratio of atomic wt.% of elements, Au–Pt	Pt electrochemically active surface area, A_r (cm ²) ^a
0 Au:40 Pt	100	12.10
10 Au:30 Pt	22.47:77.53	9.35
20 Au:20 Pt	48.97:51.03	8.23
30 Au:10 Pt	74.26:25.74	5.55

^a Measured by integrating the charge under the hydrogen adsorption/desorption peaks in cyclic voltammetry.

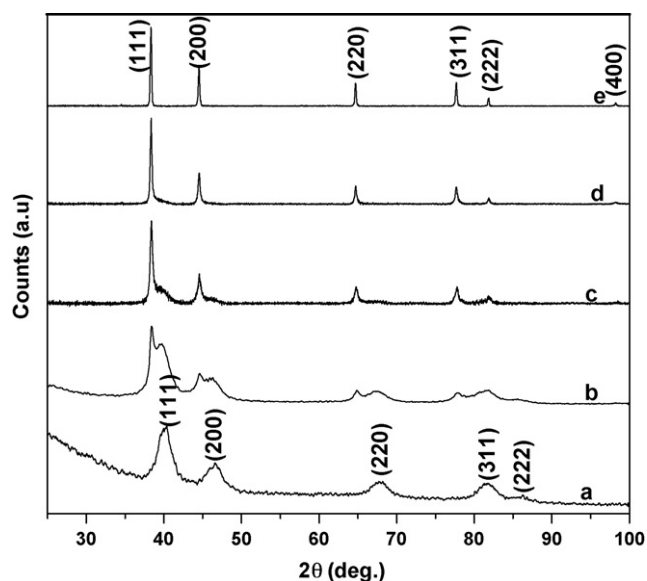


Fig. 1. XRD patterns of Au–Pt/C of various compositions: (a) (0:40); (b) (10:30); (c) (20:20); (d) (30:10); (e) (40:0).

by their indices, are observed. The diffraction patterns of the compositions: (a) Pt/C (40%), (e) Au/C (40%) show a typical face centred cubic (fcc) structure, and the corresponding structures of the pure Au and Pt bulk metals are observed. By contrast, the other compositions, viz., (b) Au–Pt/C (10%:30%), (c) Au–Pt/C (20%:20%) and (d) Au–Pt/C (30%:10%) show two sets of such reflections. This indicates condensation of two different crystalline phases although both correspond to the same crystalline structure type. These cell parameters and reflections are fairly close to those expected for their bulk metals of Au ($a = 3.923 \text{ \AA}$) and Pt ($a = 4.078 \text{ \AA}$). The invariance of the cell parameter values appears to correspond to a situation where the metallic constituents condense independently as unalloyed nanoparticles [15]. Merger of the peaks between $2\theta = 38.4^\circ$ (Au) and $2\theta = 39.88^\circ$ (Pt) further indicates that the nanoparticles are bimetallic in nature, as observed by Wu et al. [16].

The TEM images and the corresponding particle-size distribution histogram constructed from the data collected from 500 nanoparticles of various compositions of Au–Pt/C unalloyed bimetallic nanoparticles are shown in Fig. 2 for (a) 0:40, (b) 10:30, and (c) 20:20 Au–Pt/C. The Pt and Au nanoparticles are uniformly dispersed on the Vulcan carbon support and their size distribution is fairly narrow. The average size of the particles is approximately 5–6 nm, irrespective of the composition. Upon magnification, the corresponding TEM images of Au–Pt/C unalloyed

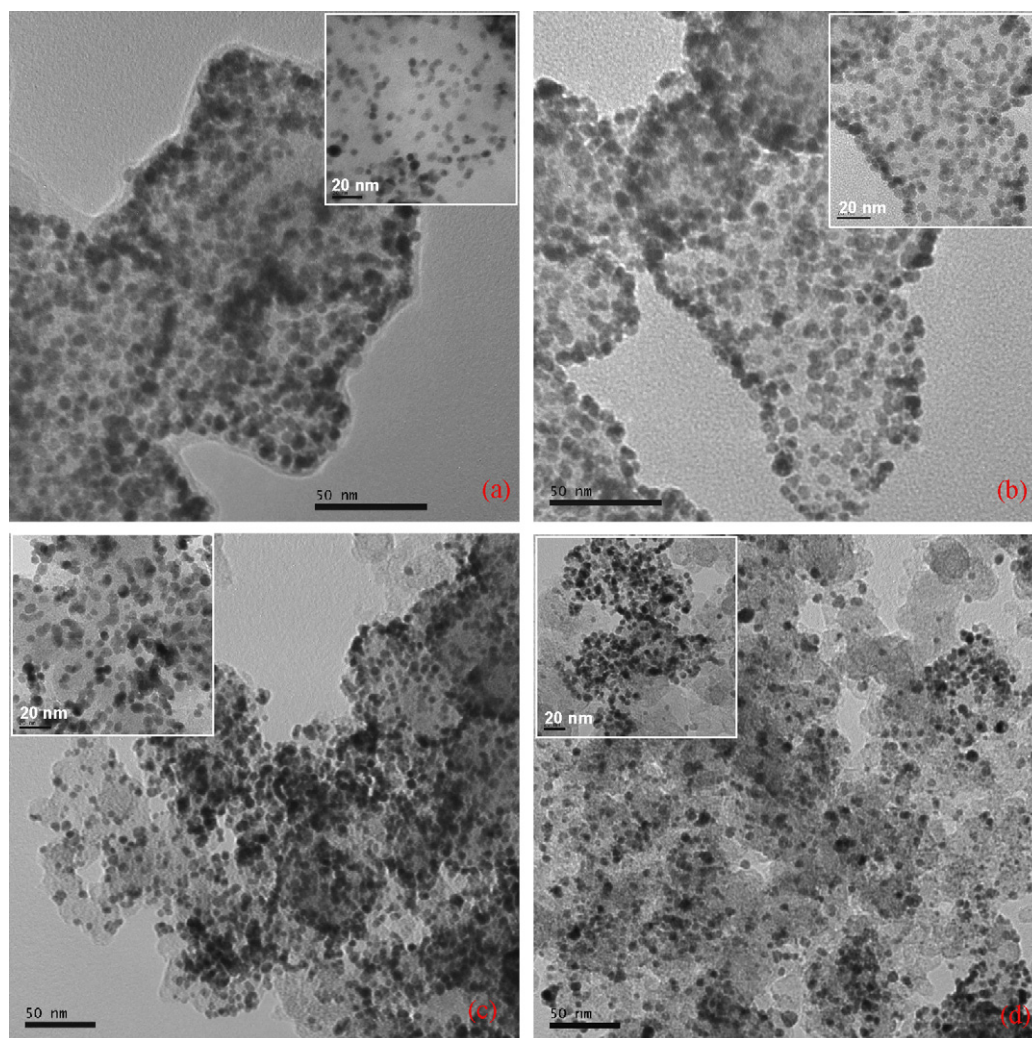


Fig. 2. TEM images (inset: higher magnification) and corresponding particle-size distribution histograms of Au–Pt/C with various loading levels: (a) 0:40; (b) 10:30; (c) 20:20; (d) 30:10.

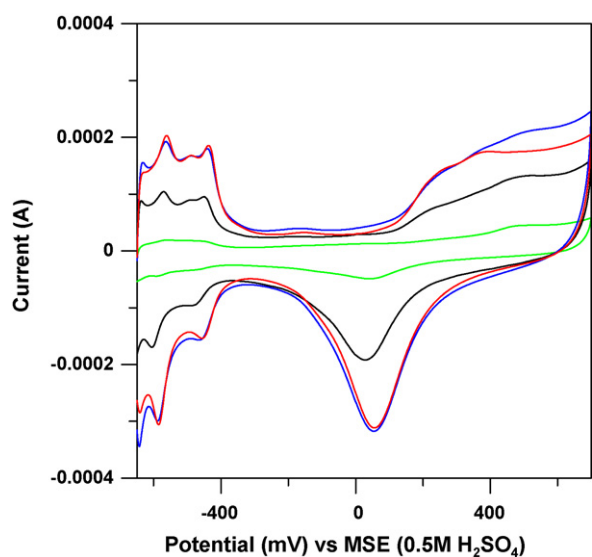


Fig. 3. Cyclic voltammograms of Au–Pt/C bimetallic nanoparticles recorded in 0.5 M H₂SO₄ solution at a scan rate of 0.05 V s⁻¹: () (0:40), () (10:30), () (20:20), () (30:10).

bimetallic nanoparticles clearly show uniform spherical or elliptical shapes.

Cyclic voltammetry was performed in 0.5 M H₂SO₄ solution over a potential region of –0.65 to 0.65 V and at a scan rate of 0.05 V s⁻¹ for obtaining the surface composition and the characteristics of Au–Pt/C bimetallic nanoparticles immobilized on the GC surface (Fig. 3). The voltammetric profile showed Pt oxide formation and reduction peaks, as well as the characteristic hydrogen adsorption waves. Further, a stable response was obtained after a few potential cycles and no oxidation/reduction current from Au was observed within this potential scan. Reduction in the charge corresponding to hydrogen adsorption/desorption on the Pt surface is observed with increase in the atomic ratio of Au loading (and an associated decrease in Pt loading). The predominance of the current response in the metal (Pt or Au) oxidation region and the absence of a response specific to Au may be indicative of (i) the surface being enriched with Pt; or (ii) the ‘oneness’ of Au–Pt arising from interactions stabilizing Au atoms on the particle surface with adjacent Pt atoms [10].

The platinum active surface area A_r (cm²) was estimated by integrating the charge Q_H in the adsorption–desorption region of hydrogen in the potential range between –0.65 and 0.3 V, assuming that hydrogen is adsorbed on Pt sites and not on Au particles [17]. Then, the charge is calculated by the following equation:

$$Q_H = \frac{Q_{\text{total}} - Q_{\text{DC}}}{2} \quad (1)$$

$$A_r = \frac{Q_H}{210} \quad (2)$$

where Q_{total} is the absolute value of the charge corresponding to the anodic and cathodic region of hydrogen adsorption–desorption, and Q_{DC} is the double-layer capacitive charge in terms of μC . By assuming a charge of 210 $\mu\text{C cm}^{-2}$ for the adsorption of a monolayer of hydrogen [18], the active surface area was calculated from Eq. (2). The results are shown in Table 1.

Linear sweep polarization curves for the ORR obtained using a rotating disc electrode configuration at 900 rpm on various compositions of Au–Pt/C bimetallic nanoparticles in O₂-saturated 0.5 M H₂SO₄ are presented in Fig. 4. The curve for the commercial 40% Pt/C (E-Tek) sample is also included for the sake of comparing the

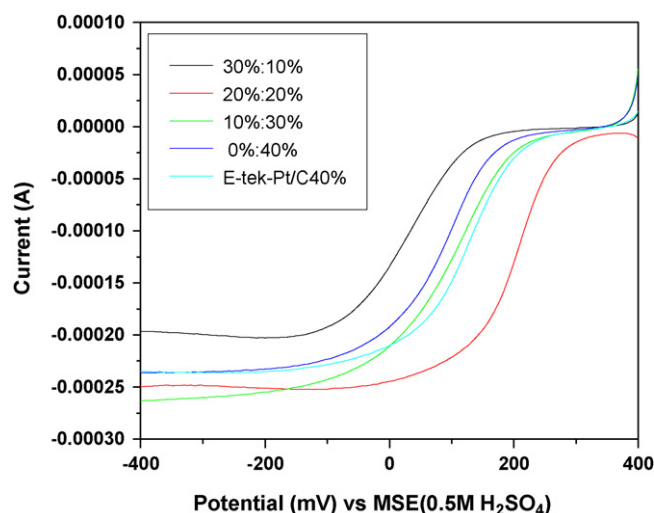


Fig. 4. Linear sweep voltammograms recorded in O₂-saturated 0.5 M H₂SO₄ solution at 900 rpm for Au–Pt/C bimetallic nanoparticles: () (30:10); () (20:20); () (10:30); () (0:40); () (E-tek-Pt/C 40) scan rate = 0.005 V s⁻¹.

efficiency of ORR activity. It should be noted that on all catalysts, the ORR is diffusion controlled when the potential is lower than 0.2 V but is under mixed diffusion-kinetic control between 0.2 and 0.4 V.

The half-wave potential values obtained from the curves in Fig. 4 for ORR with various compositions of Au–Pt/C catalysts are shown in Table 2. The data clearly show that the half-wave potential in the case of Au–Pt/C (20:20) is shifted by 0.110 V more positive (or less negative) with reference to that obtained with the Pt/C (40%–‘polyol’ sample) and Pt/C (40 E-Tek). Catalysts with an Au content in excess of the 20:20 ratio, for example, Au–Pt/C (30:10) show negative shifts in half-wave potential in comparison with both Pt/C samples (with an associated decrease in the current value). This indicates that the catalytic activity decreases with an increase in the Au content. It is important to note that the behaviour of the Au–Pt/C (10:30) sample is close to that of the Pt/C (E-Tek) sample. These results suggest that a reasonably useful catalytic activity can be derived with samples of composition between Au–Pt/C (20:20) and Au–Pt/C (10:30). It is believed that an optimum content of Au will contribute to a reduction in the Pt–OH formation that is known to ‘poison’ the catalyst for ORR [9]. If this bifunctional mechanism is taken to explain the results presented in this work and those of other researchers, the mechanism via which excess gold can be counter-productive for ORR activity requires detailed studies using surface spectroscopy.

Enhancement of Pt activity for ORR by Au nanoparticles has been recently reported [8] and is attributed to the optimum dispersion of the Pt phase on Au rather than to tuning of the electronic properties

Table 2

Comparison of half-wave potential for O₂ electroreduction, B values, and the number of electrons transferred during ORR, at Au–Pt/C bimetallic nanoparticles of various compositions.

Composition (atomic wt.%)	Half-wave potential of O ₂ reduction (mV) vs. 0.5 M MSE (0.5 M H ₂ SO ₄)	B (mA cm ⁻² rpm ^{-1/2})	n
0 Au:40 Pt	96	0.130	3.96
10 Au:30 Pt	98	0.124	3.76
20 Au:20 Pt	200	0.127	3.92
30 Au:10 Pt	50	0.114	3.47
E-tek-40(Pt/C)	100	0.128	3.99

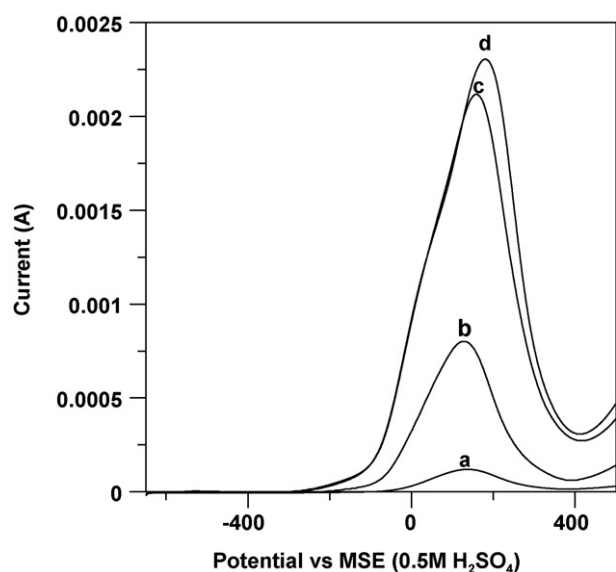


Fig. 5. Linear sweep voltammetric response of various compositions of Au-Pt/C in 0.5 M H₂SO₄ containing 0.1 M methanol at scan rate 0.005 V s⁻¹: (a) (30:10); (b) (20:20); (c) (10:30); (d) (0:40).

of Pt through interaction with the gold particles. On the other hand, Fernandez et al. [15] proposed that the superior electrocatalytic activity is due to the formation of Pt–Au alloys. In the present study, however, the unalloyed bimetallic Au–Pt particles are also found to be equally electrocatalytically active. The issue of Au–Pt being alloyed vs. unalloyed remains to be explored further in order to arrive at a definitive conclusion.

For the sake of completeness of the discussion, it may be recalled that in acid media, the Au (1 1 1) surface is hardly active as an ORR electrocatalyst [19]. This is because as Au is not capable of providing adsorption sites for the nucleation of OH_{ads} species. Such species, generated from the dissociation of water at the Pt surface in acidic electrolytes, can be considered as poisoning species in the ORR (ca. Pt–OH formation), since their presence reduces the number of active sites for the activation of oxygen via dissociative chemisorption, or splitting of the O–O bond [20]. As mentioned earlier, through a bifunctional mechanism, Au inhibits the formation of Pt–OH and thus allows Pt to act efficiently in the electrocatalytic process. The number of electrons (*n*) transferred during the ORR in an alkaline medium with gold nanoparticles of (1 0 0) orientation was reported to be 3.5 [21]. The other arguments involve the influence of Pt–Pt bond distance, in turn affected by the presence of a second metal, for example, Cr, Co, Fe or Ni [19]. An optimum Pt–Pt bond distance of 2.73 Å for ORR was reported by Mukerjee et al. [22]. In some instances, the effect of particle size on the Pt–Pt bond distance, though invoked, is not supported by experimental evidence. The issue of the effect of Pt particle size on the ORR was studied by Mayrhofer et al. [23]. The authors found that as the particle size decreases, OH coverage increases and consequently inhibits ORR.

Having found from the present studies that a certain Au–Pt composition is effective in bringing about ORR at less negative potentials, namely, Au–Pt/C (20:20), an examination was made of how the same catalyst behaves towards a competing reaction like methanol oxidation (see above), which would lower cathode catalyst performance in direct methanol fuel cells.

Steady-state, linear sweep voltammetric (LSV) responses of various compositions of Au–Pt/C catalysts in solutions containing 0.1 M methanol in H₂SO₄ at a scan rate of 0.005 V s⁻¹ are presented in Fig. 5. It can be seen that Au–Pt/C (20:20) gives a methanol oxidation current that is less than half that with Pt/C (40%). Moreover,

as the Au content is increased in Au–Pt/C (30:10), the methanol oxidation current is further reduced. It can be concluded that a reasonably good *methanol tolerance* of the catalyst can be achieved by optimizing the composition of Au and Pt from 30 to 10% and *vice versa*, respectively. It is therefore proposed that this system is a good candidate for combinatorial selection of methanol-tolerant cathode catalysts for use in direct methanol fuel cells [24].

Prompted by the near-perfect polarization characteristics of ORR on Au–Pt, details of kinetics are now under consideration. For a quantitative estimation of ORR kinetics catalyzed by various compositions of Au–Pt/C bimetallic nanoparticle catalysts, current–potential measurements at different rotation rates ranging from 200 to 2500 rpm were performed at a potential scan rate of 0.005 V s⁻¹, using a rotating glassy carbon disc (see supporting information Figure S1 below). The mass-transfer limiting currents can be observed as the electrode potential becomes more negative (i.e., 0.0 V) which indicates that the diffusion process becomes the dominant step in the electrocatalytic reaction.

In the case of thin films of supported catalysts in Nafion, the Koutecký–Levich (K–L) plots can be expressed as follows, assuming a first order reaction in oxygen species:

$$\frac{1}{i} = \frac{1}{i_k} + \frac{1}{B\omega^{1/2}} \quad (3)$$

where $B = 0.62nFD^{2/3}\nu^{-1/6}C_{O_2}$. Here, *i* is the measured current density, *i_k* is the kinetic current density, *i_L* is the diffusion (mass-transfer) limited current density, *F* is the Faraday constant, *D* is the diffusion coefficient of O₂ (1.9 × 10⁻⁵ cm² s⁻¹), ω is electrode rotation rate in unit of rpm, ν is kinematic viscosity of water (1.0 × 10⁻² cm² s⁻¹), and *C_{O₂}* is the concentration of O₂ in dilute aqueous sulfuric acid (1.1 × 10⁻⁶ mol cm⁻³). Fig. S1 (supporting information figure) shows K–L plots of *i*⁻¹ vs. $\omega^{-1/2}$ derived from hydrodynamic voltammetric measurements for various ratios of Au to Pt in the bimetallic nanoparticle at different reduction potentials in the limiting current region.

The *B* values and the number of electrons transferred during the ORR are shown in Table 2.

The *B* values measured from the slopes of the plots (Fig. S1) are 0.130, 0.124, 0.127, and 0.114 mA cm⁻² rpm^{-1/2}. These are in good agreement with those corresponding to *n* = 4 involved in the ORR [25]. This indicates a direct pathway for the reduction of oxygen to water.



Insights into the efficiency of the electrocatalysts can be obtained from the value of *n*. Additionally, it is interesting to note that the presence of Au to an extent of nearly 75% of the bimetallic composition (Au–Pt/C (30:10)) does not change the mechanism of oxygen reduction. This catalyst is also associated with a relatively low activity for methanol oxidation reaction. A combination of these two features, namely, ORR activity and inhibition of methanol oxidation appears to offer a promising methanol-tolerant cathode catalyst for direct methanol fuel cells. It is believed that the presence of gold reduces the Pt activity for the dehydrogenation step in methanol oxidation, either by a geometric effect or by a synergism operating between Au and Pt.

Adzic et al. [10] suggested that the ORR activity of Au cluster-modified Pt nanoparticles is due to the electronic behaviour of the surface of the cathode that prevents platinum atoms from dissolving in the electrolyte, while leaving the overall oxygen splitting activity of the platinum unchanged. The results presented in this work, in conjunction with those reported by various researchers suggest that there is a need to balance the ORR activity and methanol tolerance by adjusting the % composition of Au and Pt in the prepared catalysts. More recently, Wells et al. [26] have

discussed the issue of alloying in the case of PtCr/C and its influence on the ORR activity. In this work, it was found that when the formation of the alloy is restricted to the surface of the catalyst nanoparticles, only a limited enhancement of ORR can be observed. Whereas, when the bulk alloy phase is present, the specific activity of the catalyst increases to 2–3.5 times that of the Pt/C catalyst. These results highlight the importance of the alloyed and unalloyed phases. In unpublished work, we have shown that Au–Pt nanoparticles synthesized using polyol protocol in presence of a certain class of stabilizers, are alloyed in nature but exhibit inferior electrocatalytic activity towards ORR, in contrast to the observations of Fernandez et al. [15]. These samples have features corresponding to a core (Pt)–shell (Au) arrangement in UV–vis spectroscopic studies that need to be supplemented with microscopic and surface analyses to provide structure–property relationships. We are currently focusing our attention on such case studies.

4. Conclusions

Nanoparticles of Au–Pt/C have been prepared via a synthetic procedure involving a polyol method that leads to the formation of Au–Pt/C nanoparticles of 5–6 nm average particle size. This method entails refluxing a mixture of the individual metal salts at 85 °C in ethylene glycol with Vulcan carbon. At this temperature, ethylene glycol acts as both a solvent and a reducing agent, while porous carbon immobilizes the metal nanoparticles. Powder X-ray diffraction analysis reveals the formation of unalloyed bimetallic nanoparticles. The catalytic behaviour of the unalloyed bimetallic nanoparticles towards structure-sensitive reactions like the electroreduction of oxygen and methanol oxidation has been examined in this study.

The electrocatalytic activity of unalloyed Au–Pt/C bimetallic nanoparticles towards the ORR has been evaluated from steady-state polarization measurements. Rotating disk electrode (RDE) measurements indicate that a direct four-electron transfer mechanism is mainly followed for ORR on unalloyed Au–Pt/C bimetallic nanoparticles for all compositions examined. The half-wave potential for the ORR on unalloyed bimetallic Au–Pt/C (1:1) is approximately 100 mV less negative compared to that of Pt/C (home-made and E-Tek). Methanol oxidation on catalysts with compositions ranging from 0:40 to 30:10 (Au:Pt) has been investigated. The Au:Pt/C (20:20) catalyst has high ORR activity while also displaying an inhibitive effect towards methanol oxidation.

Acknowledgements

KLNP thanks the Department of Science & Technology, India for financial assistance through a grant-in-aid programme

[SR/S1/PC-37/2004]. SSK acknowledges the award of senior research fellowship by CSIR, India. The authors thank Dr. Prakash for help in acquiring TEM images and Prof. A.K. Shukla for encouragement.

Appendix A. Supplementary data

Supplementary data associated with this article can be found, in the online version, at doi:10.1016/j.jpowsour.2008.10.121.

References

- [1] H. Sinfelt, *Bimetallic Catalysts: Discoveries, Concepts and Applications*, Wiley, New York, 1983.
- [2] A. Wieckowski, E.R. Savinova, C.G. Vayenas, *Catalysis and Electrocatalysis at Nanoparticle Surfaces*, Marcel Dekker, Inc., New York, 2003.
- [3] M.M. Maye, N.N. Kariuki, J. Luo, L. Han, P. Njoki, L. Wang, Y. Lin, H.R. Naslund, C.-J. Zhong, *Gold Bull.* 37 (2004) 217–224.
- [4] G.C. Bond, C. Louis, D.T. Thompson, "Catalysis by Gold", *Catalytic Science Series*, vol. 6, Imperial College Press, London, 2006.
- [5] D.T. Thompson, *Platinum Met. Rev.* 48 (2004) 169–172.
- [6] J.L. Fernandez, D.A. Walsh, A.J. Bard, *J. Am. Chem. Soc.* 127 (2005) 357–365.
- [7] J.L. Fernandez, V. Raghuvver, A. Manthiram, A.J. Bard, *J. Am. Chem. Soc.* 127 (2005) 13100.
- [8] D. Zhao, B.-Q. Xu, *Angew. Chem. Int. Ed.* 45 (2006) 4955–4959.
- [9] J. Luo, P.N. Njoki, Y. Lin, L. Wang, C.J. Zhong, *Electrochem. Commun.* 8 (2006) 581–587.
- [10] J. Zhang, K. Sasaki, E. Sutter, R.R. Adzic, *Science* 315 (2007) 220–222.
- [11] E.R. Cable, R.E. Schaak, *Chem. Mater.* 17 (2005) 6835–6841.
- [12] C. Liu, X. Wu, T. Klemmer, N. Shukla, X. Yang, D. Weller, *J. Phys. Chem. B* 108 (2004) 6121–6123.
- [13] D.I.G. Gutierrez, C.E.G. Wing, L. Giovanetti, J.M.R. Lopez, F.G. Requejo, M.J. Yacamán, *J. Phys. Chem. B* 109 (2005) 3813–3821.
- [14] L. Colmenares, Z. Jusys, R.J. Behm, *J. Phys. Chem. C* 111 (2007) 1273–1283.
- [15] P.H. Fernandez, S. Rojas, P. Ocon, J.L.G. Fuente, J.S. Fabian, J. Sanza, M.A. Pena, F.J.G. Garcia, P. Terreros, J.L.G. Fierro, *J. Phys. Chem. C* 111 (2007) 2913–2923.
- [16] M.-L. Wu, D.-H. Chen, T.-C. Huang, *Chem. Mater.* 13 (2001) 599–606.
- [17] R.C. Koffi, C. Coutanceau, E. Garnier, J.-M. Leger, C. Lamy, *Electrochim. Acta* 50 (2005) 4117–4127.
- [18] V.S. Bakotzky, Y.B. Vassilyev, *Electrochim. Acta* 12 (1967) 1323–1343.
- [19] R. Adzic, J. Lipkowski, P.N. Ross, *Electrocatalysis*, Wiley-VCH, Weinheim, Germany, 1998.
- [20] M. Teliska, V.S. Murthi, S. Mukerjee, D.E. Ramaker, *J. Electrochem. Soc.* 152 (2005) A2159–A2169.
- [21] J. Hernández, J. Solla-Gullon, E. Herrero, A. Aldaz, J.M. Feliu, *J. Phys. Chem. B* 109 (2005) 12651–12654.
- [22] S. Mukerjee, S. Srinivasan, M.P. Soriaga, J. McBreen, *J. Electrochem. Soc.* 142 (1995) 1409–1422.
- [23] K.J.J. Mayrhofer, B.B. Blizanac, M. Arenz, V.R. Stamenkovic, P.N. Ross, N.M. Markovic, *J. Phys. Chem. B* 109 (2005) 14433–14440.
- [24] J. Wang, G. Yin, G. Wang, Z. Wang, Y. Gao, *Electrochem. Commun.* 10 (2008) 831–834.
- [25] H. Ye, R.M. Crooks, *J. Am. Chem. Soc.* 129 (2007) 3627–3633.
- [26] P.P. Wells, Y. Qian, C.R. King, R.J.K. Wiltshire, E.M. Crabb, L.E. Smart, D. Thompsett, A.E. Russell, *Faraday Discuss.* 138 (2008) 273–285.